Synthesis and Characterization of High-Spin Iron(III) 2-Hydroxy-5,10,15,20-tetraphenylporphyrin. The Unprecedented Example of the Cyclic Iron Porphyrin Trimer†

Jacek Wojaczyński and Lechosław Latos-Grażyński*

Institute of Chemistry, University of Wrocław, 14 F. Joliot-Curie St., Wrocław 50 383, Poland

Received May 10, 1994[⊗]

The oligomerization process of a monomeric iron(III) 2-hydroxy-5,10,15,20-tetraphenylporphyrin complex, (2-OH-TPP)$Fe^{III}Cl$, affords the unprecedented cyclic trimeric complex [(2-O-TPP)Fe^{III}]$_3$. The spectroscopic evidences indicate that this compound has a head-to-tail cyclic trimeric structure with the pyrrolic-alkoxide groups forming bridges from one macrocycle to the iron(III) ion in the adjacent macrocycle PFe−O−PFe−O−PFe−O. The inherent optical asymmetry of the basic oligomerization (2-OH-TPP)Fe^{III}− unit leads to formation of the enantiomeric iron(III) porphyrin trimers. The ^{1}H NMR spectrum of trimeric [(2-O-TPP)Fe^{III}]$_3$ is presented and analyzed. The presence of the three paramagnetic, weakly coupled high-spin iron(III) centers produces marked variation of positions and line widths for the pyrrole resonances. The characteristic upfield positions of the 3-H pyrrole resonances were determined and considered as the diagnostic feature for the iron(III)−pyrrole alkoxide coordination. The large upfield contribution to the 3-H pyrrole contact shift was accounted for by the donation of the electron density from the 2-oxygen on the half-occupied d_{z^2} orbital of the external iron(III) ion. [(2-O-TPP)Fe^{III}]$_3$ was cleaved by protic acids (HX) to form high-spin, five-coordinate species (2-OH-TPP)Fe^{III}X whose ^{1}H NMR spectra were analyzed. The stepwise cleavage mechanism was determined in the course of the titration with TFA. The process involved the formation of a linear dimeric intermediate [(2-OH-TPP)Fe^{III}−(2-O-TPP)-Fe^{III}(TFA)]. Addition of an excess of oxygen base (methoxide ion, hydroxide ion in methanolic solutions) to a solution of [(2-O-TPP)Fe^{III}]$_3$ in chloroform-*d* resulted in the conversion to the five-coordinate, high-spin complexes [(2-O-TPP)Fe^{III}X]$^-$ (X = CH_3O^-, OH^-). The base-catalyzed exchange of the proton at the position next to the hydroxy group (3-H) was observed for [(2-O-TPP)Fe^{III}X]$^-$ species due to the keto−enol tautomerism. The characteristic shifts of the 3-H resonances in [(2-O-TPP)Fe^{III}(OH)]$^-$ (33.4 ppm), (2-OH-TPP)Fe^{III}Br (79.1 ppm), and (2-benzoyloxy-TPP)Fe^{III}Cl (91.4 ppm) provided direct insight into the electronic structure of tautomeric forms.

Introduction

Coordinating properties of porphyrins, widely used in biomimetic chemistry and catalytic studies, can be remarkably modified by introduction of some additional metal ion coordinating centers at the porphyrin periphery. Such substituents are suitable for coordination of the metal ion of the same or other molecular systems.[1] These "hybrid" bifunctional ligands combine properties of the porphyrin macrocycles with those of the peripheral coordinating moiety.

The monohydroxy-substituted octaethylporphyrin and tetraphenylporphyrin are the representative examples of polyfunctional ligands related to porphyrins. They are able to coordinate by using tetranitrogen macrocyclic center and/or by using an ionized hydroxyl group of the periphery. Three structurally distinct locations of the hydroxyl substituents, for originally highly symmetrical model porphyrins $OEPH_2$ and $TPPH_2$, are synthetically attainable: a *meso* position for $OEPH_2$ and β-pyrrole or phenyl positions for $TPPH_2$.[2−5] Insertion of iron in 5-(2-hydroxyphenyl)-10,15,20-tritolylporphyrin ($TTOPH_2$) or in 5-hydroxyoctaethylporphyrin (oxophlorin, $OEPOH_2$) results in the formation of the high-spin iron(III) doubly oxo bridged head-to-tail dimers, [(TTOP)Fe^{III}]$_2$ and [(OEPO)Fe^{III}]$_2$, respectively (Chart 1), in which iron(III) centers are weakly antiferromagnetically coupled.[6,7]

The structure of [(TTOP)Fe^{III}]$_2$ was determined by X-ray crystallography and the retention of the dimeric structure in solution was demonstrated by ^{1}H NMR spectroscopy.[6] Dimerization through phenoxide ([(TTOP)Fe^{III}]$_2$) or *meso* oxygen ([(OEPO)Fe^{III}]$_2$) rather than μ-oxo bridging was preferred in both cases.[6,7] Goff et al. characterized the manganese(III) dimer [(TTOP)Mn^{III}]$_2$ and detected, by means of ^{1}H NMR, the diphenoxo bridged heteronuclear complex [(TTOP)Fe^{III}(TTOP)-Mn^{III}].[6b]

Iron oxophlorin complexes are significant in context of their involvement as intermediates in the conversion of iron porphyrin

* Author to whom correspondence should be addressed.

† Abbreviations used: P, porphyrin dianion; TPP, 5,10,15,20-tetraphenylporphyrin dianion; OEP, octaethylporphyrin dianion; TTOP, 5-(2-hydroxyphenyl)-10,15,20-tritolylporphyrin trianion; OEPO, 5-hydroxyoctaethylporphyrin (oxophlorin) trianion; Etio I O, trianion of oxophlorin derived from etioporphyrin I; 2-OH-TPP, dianion of 2-hydroxy-5,10,15,20-tetraphenylporphyrin; 2-O-TPP, trianion of 2-hydroxy-5,10,15,20-tetraphenylporphyrin; 2-OH-TPP-d_{20}, dianion of 2-hydroxy-5,10,15,20-tetraphenylporphyrin deuterated at *meso* phenyl positions; 2-OH-TPP-d_8, dianion of 2-hydroxy-5,10,15,20-tetraphenylporphyrin deuterated at not substituted pyrrole rings; 2-O-TPP-d_{20} and 2-O-TPP-d_8, corresponding deuterated trianions; 2-BzO-TPP, dianion of 2-benzoyloxy-5,10,15,20-tetraphenylporphyrin.

⊗ Abstract published in *Advance ACS Abstracts,* January 15, 1995.

(1) Morgan, B.; Dolphin, D. *Struct. Bonding* **1987**, *64*, 115.
(2) Barnett, G.; Hudson, M. F.; Combie, S. W.; Smith, J. M.; *J. Chem. Soc., Perkin Trans. 1* **1973**, 69.
(3) Little, R. G.; Anton, J. A.; Loach, P. A.; Ibers, J. A. *J. Heterocycl. Chem.* **1975**, *12*, 343.
(4) Callot, H. *Bull. Soc. Chim. Fr.* **1974**, 1492.
(5) Crossley, M. J.; King, L. G.; Pyke, S. M. *Tetrahedron* **1987**, *43*, 4569.
(6) (a) Goff, H. M.; Shimomura, E. T.; Lee, Y. J.; Scheidt, W. R. *Inorg. Chem.* **1984**, *23*, 315. (b) Godziela, G. M.; Tilotta, D.; Goff, H. M. *Inorg. Chem.* **1986**, *25*, 2142.
(7) Masuoka, N.; Itano, H. A. *Biochemistry* **1987**, *26*, 3672.

0020-1669/95/1334-1044$09.00/0

Chart 1

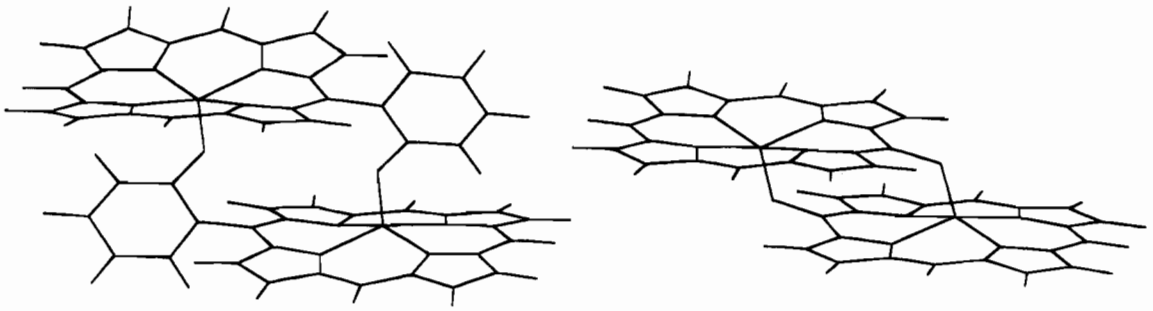

$[(TTOP)Fe^{III}]_2$ $[(OEPO)Fe^{III}]_2$

Scheme 1

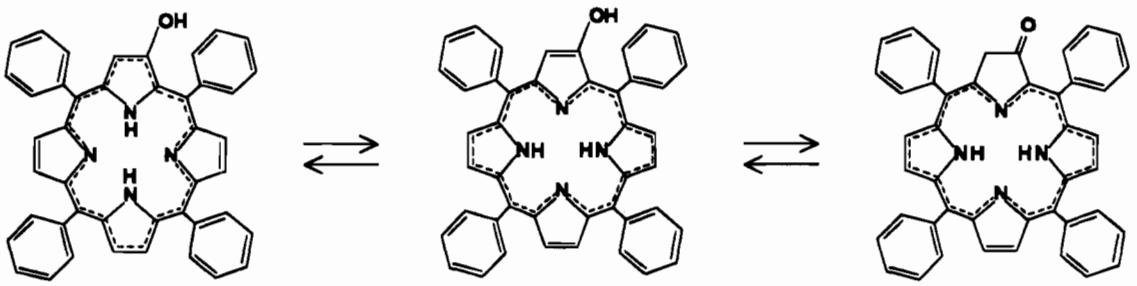

to billiverdin in the oxidative heme destruction.[8] Matsuoka and Itano characterized the iron(III) oxophlorin dimer $[(OEPO)Fe^{III}]_2$ by a range of spectroscopic techniques.[7] The presence of two paramagnetic centers produced marked changes of the ^1H NMR spectral parameters as compared to monomeric analogs including variation of the line widths for the methylene protons.[9] Recently, the formation of $[(OEPO)Mn^{III}]_2$ was demonstrated.[10] The unique structure of the related indium complex was determined by X-ray crystallography.[11] Two isomers were identified for the $[(Etio\ I\ O)Fe^{III}]_2$ dimer. The existence of isomers reflects the lower symmetry of the high-spin monomeric (Etio I OH)$Fe^{III}Cl$ unit as compared to (OEPOH)$Fe^{III}Cl$.[9]

The 2-hydroxy-5,10,15,20-tetraphenylporphyrin is the tetraphenylporphyrin derivative hydroxylated at one β-position. An equilibrium (Scheme 1) between aromatic hydroxyl, enol, and keto tautomers was determined by Crossley et al.[5,12-15]

The properties of β-hydroxytetraphenylporphyrin were discussed in the context of the π-delocalization and the complex tautomeric equilibria which also include the NH tautomerism at the pyrrolic nitrogens.[5,12-15] Complexes of 2-hydroxytetraphenylporphyrin have received relatively little systematic study. They were synthesized as the intermediate species in the hydroxylation procedure.[4,5] The insertion of nickel(II), copper(II) and zinc(II) in β-hydroxytetraphenylporphyrin stabilized tautomers with a hydroxy group at the β-position.[14] To the best of our knowledge complexes of trivalent metal ions with 2-hydroxytetraphenylporphyrin have not been previously characterized.

Here we present the results of our studies on an oligomerization of iron(III) β-hydroxy-substituted iron(III) tetraphenylporphyrin to form an unprecedented cyclic trimeric complex. ^1H NMR spectroscopy provides a uniquely useful probe for studying the structure of iron porphyrins in solution.[16,17] The hyperfine shift patterns are particularly sensitive to the spin ligation and oxidation state of the metal. The diiron(III) porphyrins bridged by ligands containing an oxygen atom(s) presented ^1H NMR spectroscopic patterns unequivocally accountable by their dimeric structures.[5,9,18-22] In this paper we report a detailed examination of the ^1H NMR spectra of trimeric iron porphyrin with a particular attention to its electronic structure and to a comparison with data obtained for a monomeric iron (III) 2-hydroxytetraphenylporphyrin complex.

Results and Discussion

Characterization of (2-BzO-TPP)$Fe^{III}Cl$. In order to produce iron(III) 2-hydroxytetraphenylporphyrin complexes the

(8) Beale, S. *Chem. Rev.* **1993**, *93*, 785.
(9) Balch, A. L.; Latos-Grażyński, L.; Noll, B. C.; Olmstead, M. M.; Zovinka, E. P. *Inorg. Chem.* **1992**, *31*, 2248.
(10) Balch, A. L.; Noll, B. C.; Reid, S. M.; Zovinka, E. P. *Inorg. Chem.* **1993**, *32*, 2610.
(11) Balch, A. L.; Noll, B. C.; Olmsead, M. M.; Reid, S. M. *J. Chem. Soc., Chem. Commun.* **1993**, 1088.
(12) Crossley, M. J.; Harding, M. M.; Sternhell, S. *J. Am. Chem. Soc.* **1986**, *108*, 3608.
(13) Crossley, M. J.; Field, L. D.; Harding, M. M.; Sternhell, S. *J. Am. Chem. Soc.* **1987**, *109*, 2335.
(14) Crossley, M. J.; Harding, M. M.; Sternhell, S. *J. Org. Chem.* **1988**, *53*, 1132.
(15) Crossley, M. J.; Burn, P. L.; Langford, S. J.; Pyke, S. M.; Stark, A. G. *J. Chem. Soc., Chem. Commun.* **1991**, 1567.
(16) La Mar, G. N.; Walker (Jensen), F. A.; In *The Porphyrins*; Dolphin, D., Ed.; Academic Press: New York, 1978; Vol. 4, p 61.
(17) Bertini, I.; Luchinat, C. *NMR of Paramagnetic Molecules in Biological Systems*; The Benjamin/Cummings Publishing Co.: Reading, MA, 1986.
(18) (a) La Mar, G. N.; Eaton, G. R.; Holm, R. H.; Walker, F. A. *J. Am. Chem. Soc.* **1973**, *95*, 63. (b) Cheng, R.-J.; Latos-Grażyński, L.; Balch, A. L. *Inorg. Chem.* **1982**, *21*, 2412. (c) Phillippi, M. A.; Goff, H. M. *J. Am. Chem. Soc.* **1982**, *10*, 6026. (d) Wysłouch, A.; Latos-Grażyński, L.; Grzeszczuk, M.; Drabent, K.; Bartczak, T. *J. Chem. Soc., Chem. Commun.* **1988**, 1377.
(19) (a) Chin, D. H.; La Mar, G. N.; Balch, A. L. *J. Am. Chem. Soc.* **1977**, *99*, 5486. (b) Chin, D. H.; La Mar, G. N.; Balch, A. L. *J. Am. Chem. Soc.* **1980**, *102*, 4344. (c) La Mar, G. N.; de Ropp, J. S.; Latos-Grażyński, L.; Balch, A. L.; Johnson, R. B; Smith, K. M.; Parish, D. W.; Cheng, R.-J. *J. Am. Chem. Soc.* **1983**, *105*, 782.
(20) Balch, A. L.; Hart, R. L.; Latos-Grażyński, L. *Inorg. Chem.* **1990**, *29*, 353.
(21) Boersma, A. D.; Goff, H. M. *Inorg. Chim. Acta* **1984**, *89*, L49.
(22) (a) Phillippi, M. A.; Baenzinger, N.; Goff, H. M. *Inorg. Chem.* **1981**, *20*, 3904. (b) Godziela, G.; Ridnour, L. A.; Goff, H. M. *Inorg. Chem.* **1985**, *24*, 1609.

Table 1. ^{1}H NMR Spectral Data[a]

compound	temp, (K)	chemical shift (ppm)				
		pyrrole-H	*meso*-phenyl *o*-H	*m*-H	*p*-H	2-OH
$[(2\text{-O-TPP})Fe^{III}]_3$	291	81.9, 77.4, 76.6, 74.7 (4H), 73.7, 72.3, 71.8, 71.4, 69.7, 69.4, 66.4 (4H), 64.1, −89.8,[b] −94.7,[b] −99.3[b]	*c* 15.0, 14.8, 14.3, 14.0, 13.3, 12.7, 12.5, 12.2, 11.9, 11.8, 10.9, 10.7, 10.5, 10.2, 9.9, 9.5, 7.0, 6.8, 6.6, 6.1, 5.5, 4.7, 4.3, 0.8, −1.2, −2.2, −4.3			
(2-OH-TPP)Fe^{III}X						
X = Cl	293	85.0, 83.1, 81.3, 79.1 (2H), 77.8, 76.4	8.5 (4H), 5.5 (4H)	13.6, 13.2 (2H), 13.0, 12.5, 12.0 (2H), 11.8	7.8, 6.7 (2H), 6.5	16.0
X = Br	293	86.1, 84.0, 82.0, 79.6, 79.1,[b] 78.5, 76.7	10.0 (4H), 6.0 (4H)	14.6, 14.1 (2H), 13.9, 13.1, 12.7 (2H), 12.5	8.3, 7.5, 6.8[d]	17.8
X = TFA	291	82.1, 78.8, 75.9, 73.6, 72.1, 70.7, 68.7	9.4 (4H), 6.7 (4H)	13.2, 12.9 (2H), 12.6, 12.2, 11.8 (2H), 11.6	8.2[d]	15.0
$[(2\text{-O-TPP})Fe^{III}(OH)]^-$	293	86.5 (2H), 77.4 (3H), 73.0, 33.4[b]	*d*			
$[(2\text{-O-TPP})Fe^{III}(OMe)]^-$	293	90.6 (2H), 81.4 (3H), 76.1, 33.7[b]	*d*			
(2-BzO-TPP)Fe^{III}Cl[e]	293	91.4,[b] 82.8, 81.3 (2H), 79.1 (2H), 78.5	8.0 (4H), 5.3 (4H)	13.3 (4H), 12.2 (3H), 11.9	6.8, 6.5 (3H)	

[a] All spectra measured in chloroform-*d*. Signal intensity given in parentheses; if not, 1H. [b] 3-H pyrrole resonance. [c] Complex multiplet (peak assignments and intensity not shown). [d] Peaks overlapped by the strong solvent signal. [e] β-Benzoyloxy resonances: *o*-H, 9.1 ppm (2H); *m*-H, 8.2 ppm (2H); *p*-H, 8.0 ppm.

β-benzoyloxy derivative (2-BzO-TPP)Fe^{III}Cl was prepared by a route that involves benzoyloxation of tetraphenylporphyrin, followed by the chromatographic separation of the product and iron insertion into 2-benzoyloxy-$TPPH_2$.[4]

$$TPPH_2 \xrightarrow[C_6H_5Cl]{(BzO)_2} 2\text{-BzO-}TPPH_2 \quad (1)$$

$$2\text{-BzO-}TPPH_2 \xrightarrow[CHCl_3,\ C_2H_5OH]{FeCl_2,\ O_2} (2\text{-BzO-TPP})Fe^{III}Cl \quad (2)$$

$(BzO)_2$ = benzoyl peroxide

The electronic spectrum of (2-BzO-TPP)Fe^{III}Cl (not shown) is typical of that high-spin iron(III) tetraphenylporphyrins.[19a,23] The ESR spectrum of (2-BzO-TPP)Fe^{III}Cl demonstrated characteristic features of this electronic state with strong $g_\perp = 6$ and weak $g_{||} = 2$ signals.[24] The β-substitution markedly lowers the symmetry of the iron(III) porphyrin from the effective C_{4v} symmetry of analogous (TPP)Fe^{III}Cl. There are seven unequivalent pyrrole positions. This is reflected in the ^{1}H NMR spectrum of (2-BzO-TPP)Fe^{III}Cl (Figure 1, Table 1). One of the pyrrole resonances occurs ca. 10 ppm downfield with respect to the center of the other six pyrrole resonances. The position of the center is typical for high-spin iron(III) tetraphenylporphyrins. By comparison to other β-substituted high-spin iron(III) tetraphenylporphyrins, we have assigned this most downfield resonance to the 3-H proton.[23,25] The splitting of phenyl resonances reflects the porphyrin asymmetry. The slightly paramagnetically shifted β-benzoyloxy resonances have been assigned in the spectrum of (2-BzO-TPP-d_{20})Fe^{III}Cl (Figure 1, Trace C).

A reaction of benzoyl peroxide with TPPFe^{III}Cl (toluene-d_8, 373 K) has been followed by ^{1}H NMR spectroscopy. Apart from the typical spectral pattern of the substrate TPPFe^{III}Cl, we have easily identified the pyrrole resonances of the direct benzoylation product, i.e. (2-benzoyloxy-TPP)Fe^{III}Cl (Figure 1, Trace A′). We have not attempted to apply this procedure on the synthetic scale. However, we have found it important to

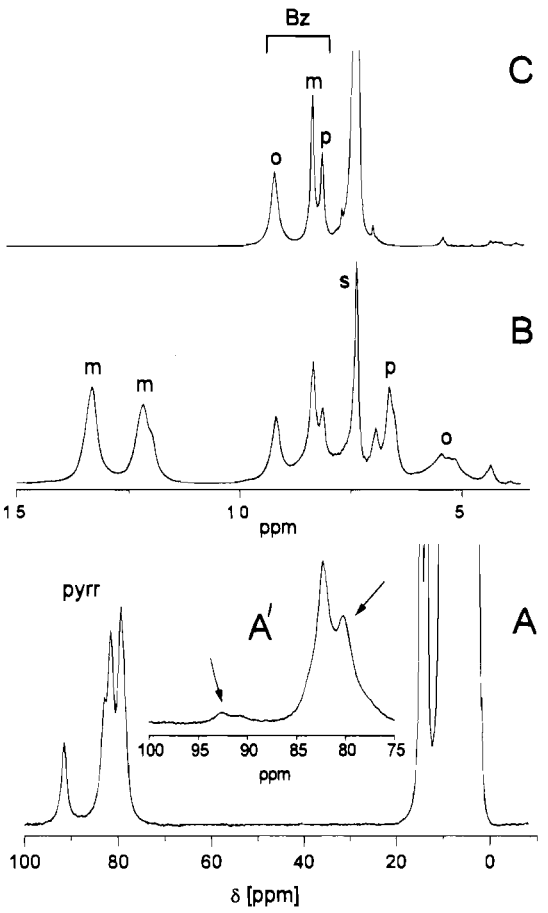

Figure 1. 300 MHz ^{1}H NMR spectrum of (2-BzO-TPP)Fe^{III}Cl in chloroform-*d* solution at 293 K. Trace A is the entire spectrum while B shows an expansion of the *meso* phenyl and β-benzoyloxy resonances. Trace C presents the similar fragment as trace B for (2-BzO-TPP-d_{20})Fe^{III}Cl. Inset A′ presents the pyrrole resonance region of the sample obtained in the course of the direct β-substitution of (TPP)Fe^{III}Cl with benzoyl peroxide in toluene-d_8 at 373 K. The spectrum was measured at 293 K in toluene-d_8. Arrows identify the pyrrole resonances of the β-substituted form(s). Resonance assignment: pyrr, pyrrole; o, m, or p, ortho, meta or para phenyl; Bz, benzoyl; s, solvent.

(23) Małek, A.; Latos-Grażyński, L., Bartczak, T. J.; Żądło, A. *Inorg. Chem.* **1991**, *30*, 3222.
(24) Palmer, G. In *The Porphyrins*; Dolphin, D., Ed.; Academic Press: New York, 1979; Vol. 4, pp 313−353.
(25) Rachlewicz, K.; Latos-Grażyński, L. *Inorg. Chem.* **1995**, *34*, 718.

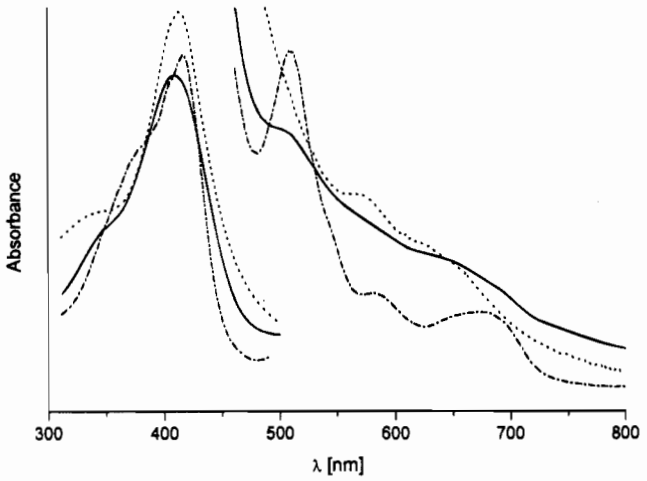

Figure 2. Electronic absorption spectra of dichloromethane solutions: (—) $[(2\text{-O-TPP})Fe^{III}]_3$; (— • —) $(2\text{-OH-TPP})Fe^{III}Cl$; (- -) $[(2\text{-O-TPP})Fe^{III}(OH)]^-$.

present its feasibility since, in all probability, it is one of the iron porphyrin degradation routes during catalytic processes.

Synthesis and Characterization of $[(2\text{-O-TPP})Fe^{III}]_3$. Ethanolysis of $(2\text{-BzO-TPP})Fe^{III}Cl$ resulted in the formation of the unprecedented trimeric molecule:

$$3(2\text{-BzO-TPP})Fe^{III}Cl \xrightarrow{NaOH/EtOH;\ H_2O} [(2\text{-O-TPP})Fe^{III}]_3 \quad (3)$$

$[(2\text{-O-TPP})Fe^{III}]_3$ has been characterized by a range of the spectroscopic methods. The electronic spectrum of $[(2\text{-O-TPP})Fe^{III}]_3$ is presented in Figure 2 (Trace A) together with the spectra of $(2\text{-OH-TPP})Fe^{III}Cl$ and $[(2\text{-O-TPP})Fe^{III}(OH)]^-$ (vide infra). The electronic spectra of $(2\text{-OH-TPP})Fe^{III}Cl$ (Trace B) and $(2\text{-BzO-TPP})Fe^{III}Cl$ (discussed previously) are typical for high-spin iron(III) tetraphenylporphyrins. The electronic spectrum of $[(2\text{-O-TPP})Fe^{III}]_3$ differs considerably from those of its precursors and from any those of five-coordinate iron(III) tetraphenylporphyrin with the oxygen donor at the axial position.[5,19,26] The Soret band shows a blue shift, and all bands are broadened as compared to those observed for $(2\text{-OH-TPP})Fe^{III}Cl$. The differences may be induced by the oxygen axial ligand coordination[26] and/or from the porphyrin−porphyrin π-interaction caused by the proximity of the porphyrin rings in the close-packed trimeric structure.[27]

The infrared spectrum of solid $[(2\text{-O-TPP})Fe^{III}]_3$ demonstrates no evidence for an μ-oxo bridge which usually displays an antisymmetric Fe−O−Fe stretching vibration (ca. 850 cm^{-1}).[28] The spectral region 800−900 cm^{-1} is identical with the one found for monomeric $(2\text{-OH-TPP})Fe^{III}Cl$.

The magnetic susceptibility of $[(2\text{-O-TPP})Fe^{III}]_3$ is somewhat lower then typical of a high-spin iron(III) porphyrin. The magnetic moment as measured by the Evans technique[29] in chloroform solution at 293 K equals 5.4 ± 0.2 μ_B per iron atom. The typical value of μ (5.9 ± 0.2 μ_B) has been determined for $(2\text{-OH-TPP})Fe^{III}Cl$ generated from the original sample of $[(2\text{-O-TPP})Fe^{III}]_3$ by splitting with gaseous HCl directly in the NMR tube. The observed lowering of the magnetic moment for the trimer with respect to the monomeric high-spin iron(III) porphyrins is due to the weak antiferromagnetic coupling.

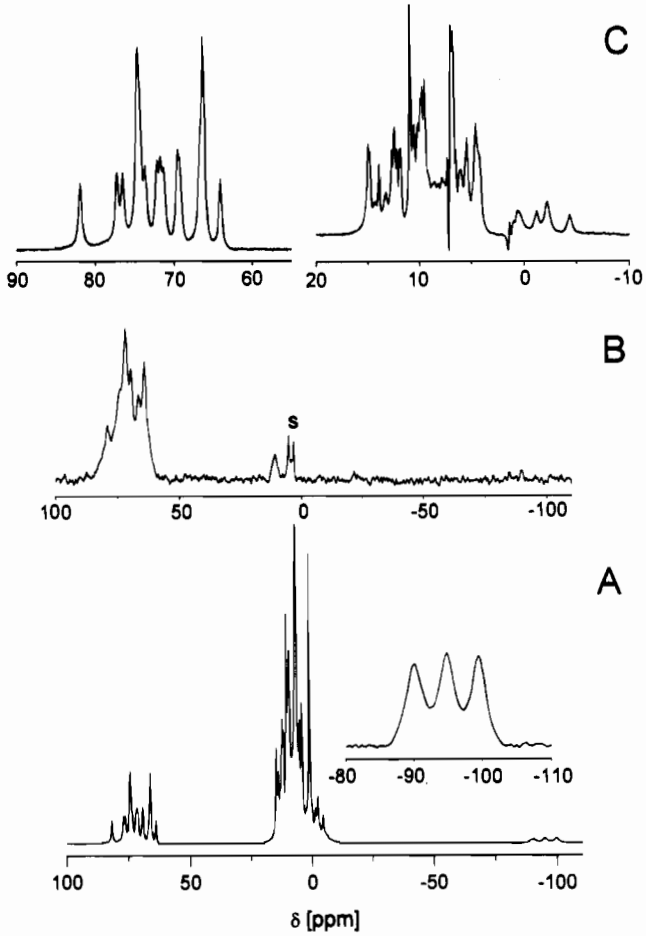

Figure 3. NMR spectra of $[(2\text{-O-TPP})Fe^{III}]_3$ at 291 K. Traces A and C show 300 MHz ^1H NMR spectra of the unlabeled sample in chloroform-*d* solution, while trace B shows the 46.06 MHz ^2H NMR spectrum in dichloromethane at 293 K for pyrrole-deuterated $[(2\text{-O-TPP-}d_8)Fe^{III}]_3$. Inset in trace A shows 3-H pyrrole resonances. Trace C shows an expansion of the downfield pyrrole resonances (55−90 ppm) and the +20 to −10 ppm region of the *meso* phenyl resonances which was obtained under T_1 inversion recovery conditions with rapidly relaxing paramagnetic resonances appearing in the normal phasing.

The Mössbauer spectrum of $[(2\text{-O-TPP})Fe^{III}]_3$ exhibits a quadrupole doublet with an isomer shift of 0.316 mm/s (vs α-Fe) and a quadrupole splitting of 0.541 mm/s demonstrated clearly at 295 K. These parameters are symptomatic of high-spin iron(III).[30]

No ESR signal was observed for $[(2\text{-O-TPP})Fe^{III}]_3$ in the sample that was frozen at 77 K in dichloromethane/toluene but typical high-spin iron(III) spectra were measured for the monomeric complexes: $(2\text{-BzO-TPP})Fe^{III}Cl$ and $(2\text{-OH-TPP})Fe^{III}Cl$. The proximity of iron(III) ions (ca. 7 Å based on the structural model) induces an efficient electron spin−spin relaxation, although magnetic coupling between the iron centers seems to be small. This results in broadening of the ESR resonances beyond detection at 77 K. This is a general feature previously found for diiron(III) porphyrins $[(TTOP)Fe^{III}]_2$ and $[(OEPO)Fe^{III}]_2$.[5,6]

The liquid matrix secondary ion mass spectrum of $[(2\text{-O-TPP})Fe^{III}]_3$ shows peaks due to the parental species $[(2\text{-O-TPP})Fe^{III}]_3$ at $(m + 1)/z = 2050$ (7%) and its stepwise deoligomerization products $[(2\text{-O-TPP})Fe^{III}]_2$ at $(m + 1)/z = 1367$ (11%)

(26) Kessel, S. L.; Hendrickson, D. N. *Inorg. Chem.* **1980**, *19*, 1883.
(27) (a) Osuka, A.; Maruyama, K. *J. Am. Chem. Soc.* **1988**, *110*, 4454. (b) Chang, C. K. *Adv. Chem. Ser.* **1979**, *173*, 162. (c) Hunter, C. A.; Sanders, J. K. M. *J. Am. Chem. Soc.* **1990**, *112*, 5525.
(28) Saxton, R. J.; Olsen, L. W.; Wilson, L. J. *J. Chem. Soc., Chem. Commun.* **1982**, 984.
(29) Evans, D. F.; James, T. A. *J. Chem Soc., Dalton Trans.* **1979**, 723.
(30) (a) Dolphin, D.; Sams, J. R.; Tsin, T. B.; Wong, K. L. *J. Am. Chem. Soc.* **1978**, *100*, 1711. (b) Hambright, P.; Bearden, A. J. In *Porphyrins and Metalloporphyrins*; Smith, K., Ed.; Elsevier: Amsterdam, 1976; p 539.

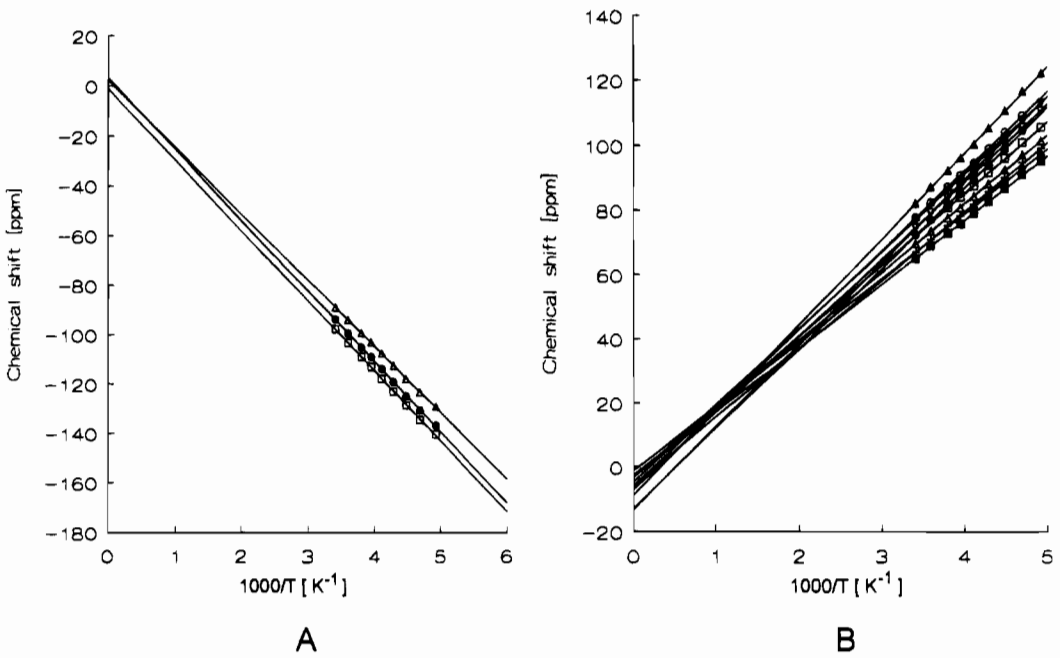

Figure 4. Curie plots of the pyrrole resonances of [(2-O-TPP)Fe^{III}]$_3$ in chloroform-*d*: (A) 3-H resonances; (B) 7,8,12,13,17,18 resonances.

and [(2-O-TPP)Fe^{III}] at $(m + 1)/z = 684$ (100%). Solely on the basis of mass spectrum, we cannot rule out even higher than trimeric oligomeric structures since larger ions might not survive in the gas phase. In our experiment the most intense peak corresponds to the monomeric unit. However, only the trimeric formula is consistent with the ^{1}H NMR data.

^{1}H NMR Spectroscopic Studies of [(2-O-TPP)Fe^{III}]$_3$. The ^{1}H NMR spectrum of [(2-O-TPP)Fe^{III}]$_3$ is shown in Figure 3. The resonance assignments, shown in Table 1, have been made on the basis of relative intensities, line width analysis and site specific deuteration. In order to identify phenyl and pyrrole resonances the ^{1}H and ^{2}H NMR spectra of [(2-O-TPP-*d*$_6$)Fe^{III}]$_3$ (deuterated at 7,8,12,13,17,18 pyrrolic positions) have been obtained. The representative ^{2}H NMR spectrum of [(2-O-TPP-*d*$_6$)Fe^{III}]$_3$ is shown in Figure 3 (trace B). The ^{2}H pyrrole resonances are readily seen. The proton resonances can be easily separated into three groups (Figure 3). The most characteristic features, three strongly upfield shifted peaks (line widths are given in parentheses) at −89.8 (675), −94.7 (690), and −99.3 (670 Hz) ppm (291 K), correspond to the 3-H pyrrole protons. The remaining pyrrole protons produce resonances in the 82−62 ppm region. Thirteen resonances, some of them partially overlapped, are present. We have applied the deconvolution procedure (not shown) to this part of the spectrum in order to demonstrate that 18 resonances of similar line widths (130−140 Hz) and the intensity of one proton each, are required to reproduce the experimental spectrum. The phenyl resonances form the complex, barely resolved pattern which is spread at the +16 to −5 ppm range (Figure 3, trace C). On the basis of the complex symmetry, 60 different phenyl resonances should be potentially traced in this region. The majority of them are located in the region usually expected for high-spin iron(III) tetraphenylporphyrins.[16,23] In addition we have found four upfield shifted phenyl resonances (−4.3, −2.2, −1.2, and +0.8 ppm), tentatively assigned to phenyl rings located close to the neighboring iron porphyrin unit.

The Curie plots for pyrrole resonances of [(2-O-TPP)Fe^{III}]$_3$ are shown in Figure 4. An attempt of the linear extrapolations demonstrates intercepts which are removed from the positions expected for the diamagnetic reference.[31] The smallest deviation has been observed for the upfield shifted pyrrole resonances. As is apparent, these dependences are not linear but demonstrate some curvature. The slight curvature of Curie plots of the downfield shifted pyrrole resonances of [(2-O-TPP)Fe^{III}]$_3$ is in the same direction as found for many monomeric high-spin iron(III) complexes.[18ab;33] Such deviations can be accounted for by the dipolar contribution to the hyperfine shifts, which has a characteristic T^{-2} dependency.[18a] The direction of curvature observed here is opposite to that seen for weakly coupled diiron porphyrins: [(OEPO)Fe^{III}]$_2$ and iron(III) porphyrin dimers with hydroquinone dianionic bridges.[9,20] The departure from the Curie law observed for [(2-O-TPP)Fe^{III}]$_3$ is a result of the zero-field splitting of individual units and clearly is not due to antiferromagnetic coupling.

The average shift of the pyrrole resonances located at the 82−62 ppm (291 K) region equals 71.8 ppm. This is slightly upfield when compared to the characteristic region for monomeric high-spin iron(III) porphyrin complexes, for instance: the average shift of the (2-OH-TPP)Fe^{III}Cl pyrrole protons equals 80.3 ppm (293 K). We relate this difference to the weak antiferromagnetic coupling between iron(III) centers of the trimer, already demonstrated in the lowering of the magnetic moment. There is a general trend in the pyrrole shifts of the antiferromagnetically coupled diiron(III) porphyrins systems. The pyrrole resonances occur higher upfield as the magnitude of the magnetic coupling between iron ions increases and a reasonable estimation of the J value based upon the pyrrole shifts was found.[20] For example for the chemical shift of the pyrrole resonance equal 72 ppm one can estimate $J = 4$ cm^{-1} in the diiron (III) porphyrin complex. Such an approach can not be directly applied to [(2-O-TPP)Fe^{III}]$_3$ because the different relation between χ (the molar susceptibility) and the J values is expected in the trimeric systems. However, the comparison of the pyrrole shift values of the diiron(III) and triiron(III) complexes sets a limit on the size of the interaction in the trimer.

(31) The chemical shifts of an analogous cyclic trimeric complex [(2-O-TPP)Ga^{III}]$_3$ have been used as a suitable diamagnetic reference.[32] The considerable ring current shifts have been found in the gallium trimer (3-H: 1.96, 2.22, 2.79 ppm; other pyrole resonances: 7.40−9.00 ppm in 293 K) but these values cannot account for the observed deviations.

(32) Wojaczyński, J.; Latos-Grażyński, L. *Inorg. Chem.* **1995**, *34*, 1054.
(33) Behere, D. V.; Birdy, R.; Mitra, S. *Inorg. Chem.* **1982**, *21*, 386.

Molecular Model of [(2-O-TPP)Fe^{III}]$_3$. Extensive attempts to obtain [(2-O-TPP)Fe^{III}]$_3$ as crystals, suitable for X-ray crystallographic studies, have not been successful. In the absence of such a data set, molecular mechanics calculations have been used to visualize the structure of the trimer and to access the degree of the porphyrin distortion that is necessary to form this species. In the minimization procedure we have used the standard MM+ parameterization of the HyperChem program with an exception of the iron coordination surroundings where we have imposed the constrains reflecting the high-spin state of the iron(III) ion. The characteristic features of the high-spin iron(III) tetraphenylporphyrins included the displacement of the iron from the plane of four nitrogens (0.45 Å) and relatively long iron−nitrogen bonds (2.05 Å).[34] The spectroscopic evidence indicated that the iron(III) complex has a head-to-tail trimeric structure, with the pyrrolic-alkoxide groups forming the bridges from one macrocycle to the metal ion of the adjacent macrocycle: PFe−O−PFe−O−PFe−O. Such an oligomeric structure accounts for the mass of the largest ion in the mass spectrometry. The ^{1}H NMR spectrum clearly points to three distinct iron(III) porphyrin units in the complex as visualized by three upfield and the multiplet of downfield pyrrole resonances. The multiplet is composed from three sets of six resonances, each corresponding to a different unit. The unprecedented upfield hyperfine shift of 3-H resonances can be explained only by the direct coordination of the β-oxygen to the external iron(III) ion as required by oligomerization. Finally, the alternative linear trimeric structure would require an OH resonance in the 15−30 ppm region, not seen for [(2-O-TPP)Fe^{III}]$_3$, and only two, instead of the observed three, 3-H pyrrole resonances in the upfield part of spectrum.

Formally high-spin iron(III) 2-hydroxy-tetraphenylporphyrin (2-OH-TPP)Fe^{III}X can be used as a building block in the oligomerization. This five-coordinate complex exists as two optical antipodes. Their structural differences may be essential to the trimer formation. 2-Hydroxytetraphenylporphyrin has a structure with two enantiotopic faces. The front and back views are not superimposable but are mirror images with respect to each other and thus this porphyrin has no inherent optical activity. However, the high-spin five-coordinate insertion product of iron(III) into 2-OH-TPPH$_2$, i.e. (2-OH-TPP)Fe^{III}X, has an optical asymmetry associated with direction of the axial ligand approach to the iron(III) ion.

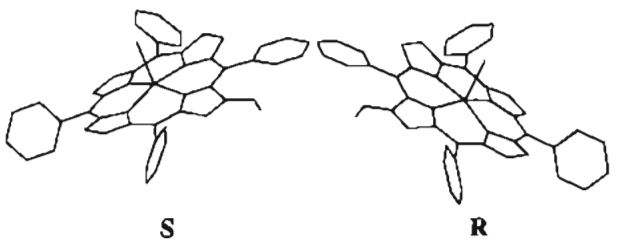

Two enantiomers of (2-OH-TPP)Fe^{III}X present the clockwise (*R*) or anticlockwise (*S*) arrangement of porphyrin β-substituents with respect to the iron(III)−axial ligand axis. The random selection of the *R* and *S* enantiomers from the enantiomeric mixture of (2-OH-TPP)Fe^{III}X to form trimers should produce the following stereoisomers: *RRR* (0.125), *RRS* (0.375), *RSS* (0.375), and *SSS* (0.125). The probabilities of the stereoisomer formation given in parentheses were calculated for the random selection of monomeric units during the trimerization. The enantiomers *RRR* and *SSS* (0.25) or *RSS* and *SRR* (0.75) would not be distinguished from each other by means of ^{1}H NMR spectroscopy. On the other hand, diastereoisomers should be easily differentiated. The *RRR* and *SSS* isomers, enatiomeric to each other, have C_3 symmetry and only one set of resonances for three identical monomeric units would be expected. A superposition of three unequivalent spectral patterns, originating from three unequivalent subunits, is anticipated for the *RSS* (*SSR*) diastereoisomer. Only the *RRS* (*SSR*) structure is consistent with the ^{1}H NMR spectrum. Schematic views of the trimeric iron(III) porphyrin skeletons as obtained by molecular mechanics are presented in Figure 5. For the sake of clarity, the phenyl rings have been omitted from the stick drawings although we have included them directly in the minimization procedure. The isomers are shown in such projections where the inertion axis is perpendicular to the plane of the figure. This inertion axis coincides with a C_3 symmetry axis of the RRR diastereoisomer or a pseudo-C_3 axis of the RRS diastereoisomer. Formally both diastereoisomers are related by a transfer of the oxygen−β-carbon bond shown by an arrow in the Figure 5. As can be seen, only moderate folding of the macrocycle and bending of the oxo substituent are required to allow for trimerization. The iron(III) ions are located at corners of the equilateral triangle at a distance of 7 Å. The space filling model, shown along with the pseudo-C_3 axis (Figure 6, A, the front view; B, the rear view) demonstrates packing of the porphyrin and phenyl rings for the *RRS* isomer. The closest contacts are in the range observed in the structures of other metalloporphyrins.[11,34] In particular, the 20-phenyl rings, exposed to the largest steric interaction (they are located close to the bridging 2-oxygen) fit perfectly into the crevice formed by three porphyrin planes.

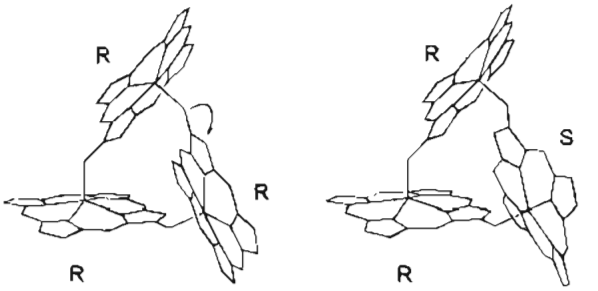

Figure 5. Drawing of two diastereoisomeric structures *RRR* and *RRS* of the trimer [(2-O-TPP)Fe^{III}]$_3$ obtained from the molecular mechanics calculations. Figure presents stick diagrams with phenyl groups and hydrogen atoms omitted for the sake of clarity. The arrow points out the necessary bond rearrangement to convert *RRR* into *RRS*.

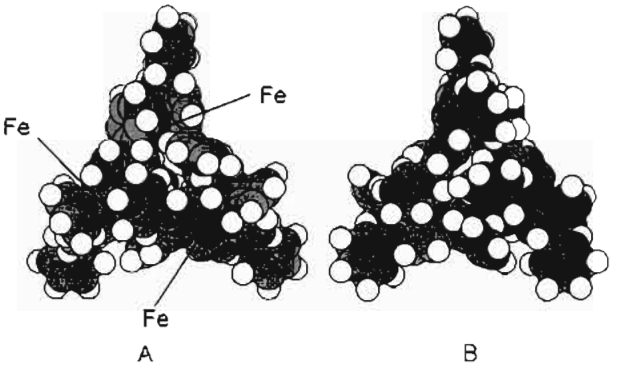

Figure 6. Space filling model of [(2-O-TPP)Fe^{III}]$_3$ (the *RRS* diastereoisomer), obtained from molecular mechanics calculations, shown in such projections where the inertion axis is perpendicular to the plane of the figure: A, the front view; B, the rear view. The model includes all atoms.

Analysis of Paramagnetic Shifts in Terms of the Structure of [(2-O-TPP)Fe^{III}]$_3$. The ^{1}H NMR spectra of [(2-O-TPP)-

(34) Scheidt, W. R., Lee, Y. J. *Struct. Bonding* **1987**, *64*, 1.

$Fe^{III}]_3$ show a number of remarkable features that must arise from its unusual molecular structure. They can be understood in the context of the presence of three high-spin iron(III) ions in the molecule. The β-hydroxy(oxo)porphyrin of each monomeric unit is coordinated simultaneously to the internal iron(III) through four nitrogens and to the external one by the oxygen. The typical delocalization pathway for high-spin iron(III) tetraphenylporphyrins gives the pyrrole resonance downfield shifts as a result of the σ-contact contribution. Additionally the π-delocalization locates a considerable amount of the spin density at the meso positions.[16,18a,b;33] The π spin density produces sign alternation of the *meso*-phenyl resonances. The dipolar contribution, caused only by the ZFS effect in high-spin iron porphyrins, is usually notably smaller than the contact contribution, and this observation has been applied in the further analysis of the hyperfine shifts.[33] We have made the simplifying but realistic assumption that for the 3-H proton the dipolar shift is given by two contributions derived from the external and internal iron(III) ions (Fe_e and Fe_i), in the absence of significant in-plane anisotropy:

$$(\Delta H/H)^{dip} = \Delta\chi[(3(\cos^2\theta_{3i}) - 1)/(r_{3i})^3 + (3(\cos^2\theta_{3e}) - 1)/(r_{3e})^3]$$

$\Delta\chi$ is the difference of the principal components of the susceptibility tensor identical for each subunit, θ_{3i} is the angle of the internal iron−3H proton vector to the z_i axis, r_{3i} is the length of this vector, θ_{3e} is the angle of the internal iron−3H proton vector to the z_e axis, r_{3e} is the length of this vector, and z_i and z_e axes are oriented along with internal or external iron(III)−oxygen bonds, respectively.

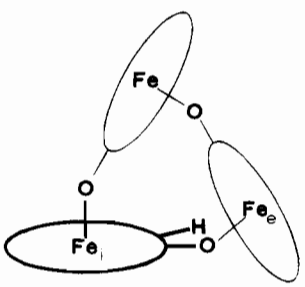

The calculations have been made using the *RRS* model. The static structure has been assumed in which $r_{3e} < r_{3i}$, but θ_{3i} is ca. 90°, and $\theta_{3e} \cong 55-56°$. This last value is close to $\theta = 54.7°$ for which the angular term of the geometric factor vanishes. The angular part of the external and internal geometric factors dictates that the estimated values of the external and internal dipolar shifts are similar and in the downfield direction. The estimate dipolar shifts are in the typical limits established for the high-spin iron(III) porphyrins.[16,18a,b;33] Hence, the upfield hyperfine shift of 3-H must be dominated by the contact mechanism. The characteristic features of the internal iron(III) influence are exemplified by ^{1}H NMR spectra of (2-OH-TPP)Fe^{III}Cl (vide infra) and (2-BzO-TPP)Fe^{III}Cl where the typical downfield set of the seven pyrrole resonances have been found. However, the presence of the second source of the spin density, i.e. the external iron(III) ion changes a sign of the hyperfine shifts for the 3-H (*R*, *R*, *S*) protons. Assuming simple additivity of contact contributions by two independent routes, we have estimated that such shift requires the downfield contribution of 70 ppm as found for (2-OH-TPP)Fe^{III}Br and the upfield one of −160 ppm. The upfield contribution to the 3-H shift results mainly from the σ-donation of the electron density of the 2-oxygen donor on the half-occupied d_{z^2} orbital of the iron(III) ion. The anticipated positive spin density on the σ-orbital of the oxygen will be directly transferred into the π-system of the pyrrole ring without any iron(III)−oxygen π-bonding. The ligand σ and π orbitals are not orthogonal, and σ-π overlap within the ligand permits the direct spin density transfer.[35,36] Considering the idealized geometry of coordination, shown below for the 2-hydroxypyrrole and phenoxide fragments, we suggest the similar delocalization mechanism to rationalize the upfield contact shifts of the protons located similarly with respect to the external iron(III) ion.

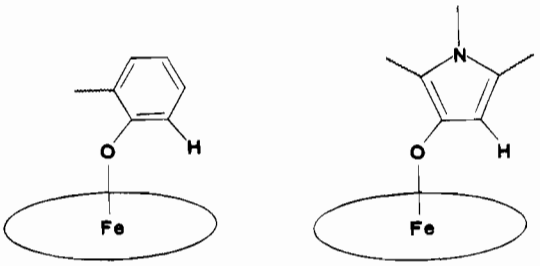

The magnitudes of the hyperfine shifts of phenoxide ortho protons in iron(III) porphyrin complexes (−90 to −150 ppm) are similar to that evaluated for the external contact contribution of 3-H protons.[37−39] The line width of the 3-H pyrrole resonances correlates with their specific locations within the trimeric structure. The dipolar contribution to line width broadening is presumed to be proportional to r^{-6} where *r* is the distance from the paramagnetic iron(III) center to the proton in question when the ligand-centered dipolar relaxation is insignificant.[39,40] The contribution from the internal iron(III) ion via dipolar and scalar mechanisms has been approximated by the line widths of downfield pyrrole resonances which vary in the rather narrow range, 130−140 Hz. The markedly larger line widths of 3-H protons (ca. 670 Hz) can be split into two parts: the internal one, which is identical to that for other pyrrole positions, and the remaining external one (ca. 530 Hz). The most likely the external one derives mainly from the dominant dipolar contribution of the closely located external iron(III) ion. The pattern of pyrrole line widths is qualitatively in agreement with the proposed molecular structure.

Cleavage of [(2-O-TPP)Fe ^{III}]$_3$ by Protic Acids. Addition of acids in excess to [(2-O-TPP)Fe^{III}]$_3$ results in cleavage of the trimer according to eq 4. Figures 7 and 8 show relevant ^{1}H

$$[(2\text{-O-TPP})Fe^{III}]_3 + 3HX \rightarrow 3(2\text{-OH-TPP})Fe^{III}X \quad (4)$$

$$X = Cl, Br, TFA$$

NMR spectra. The spectrum in Figure 7 (trace A) shows a sample of [(2-O-TPP)Fe^{III}]$_3$ to which gaseous HCl has been added. The spectrum is consistent with the formation of the racemic high-spin (2-OH-TPP)Fe^{III}Cl complex. The considerable simplification of the spectral pattern has been observed. The upfield 3-H pyrrole resonances, the most characteristic for

(35) (a) Chachaty, C.; Forchioni, A.; Ronfard-Haret, J. C. *Mol. Phys.* **1976**, *31*, 325. (b) Chachaty, C.; Rigny, P. J. *Chem. Phys.* **1982**, *79*, 203.
(36) Lisowski, J.; Latos-Grażyński, L.; Szterenberg, L. *Inorg. Chem.* **1992**, *31*, 1933.
(37) Goff, H. M.; Shimomura, E. T.; Lee, Y. J.; Scheidt, W. R. *Inorg. Chem.* **1984**, *23*, 315.
(38) Arasasingham, R. D.; Balch, A. L.; Hart, R. L.; Latos-Grażyński, L. *J. Am. Chem. Soc.* **1990**, *112*, 7566.
(39) Arasasingham, R. D.; Balch, A. L.; Cornman, C. R.; de Ropp, J. S.; Eguchi, K.; La Mar, G. N. *Inorg. Chem.* **1990**, *29*, 1847.
(40) Swift, J. In *NMR of Paramagnetic Molecules*; La Mar, G. N., Horrocks, W. D., Jr., Holm, R. H., Eds.; Academic Press: New York; 1973, p 53.

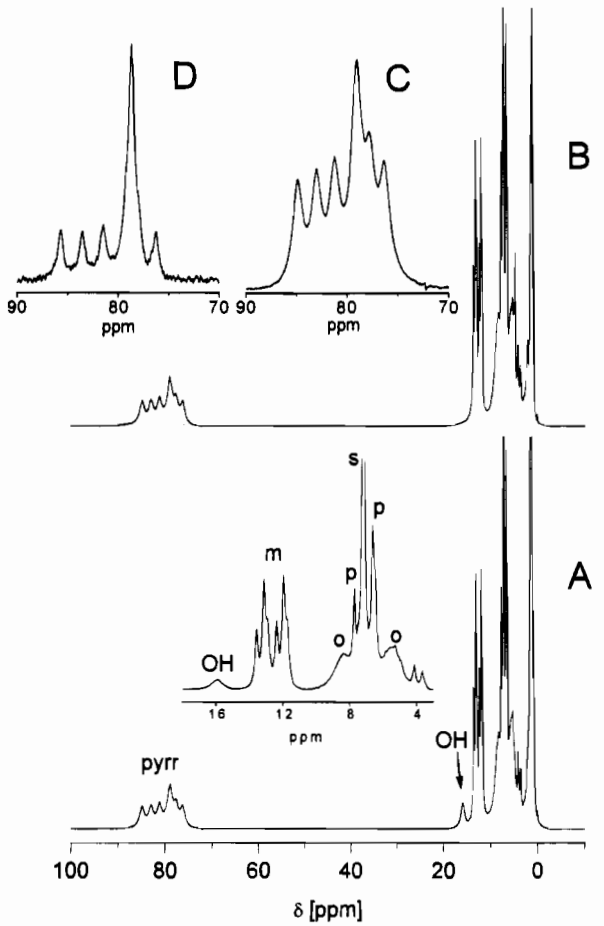

Figure 7. 300 MHz ^{1}H NMR spectrum of $[(2\text{-O-TPP})Fe^{III}]_3$ solution in chloroform-*d* after treatment with (A) gaseous HCl at 293 K and (B) gaseous HCl and D_2O. The species present in A is (2-OH-TPP)Fe^{III}Cl, and that in B is (2-OD-TPP)Fe^{III}Cl. Trace C shows the expansion of the pyrrole resonances of (2-OH-TPP)Fe^{III}Cl. The corresponding expansion of the pyrrole region of (2-OH-TPP-d_6)Fe^{III}Br is presented in trace D. Resonance assignment: pyrr, pyrrole; o, m, or p, ortho, meta or para phenyl; OH, the β-hydroxy group; s, solvent.

$[(2\text{-O-TPP})Fe^{III}]_3$, disappeared. Six new pyrrole resonances (intensity ratio 1:1:1:2:1:1) are found in the 75−85 ppm region. They correspond to seven pyrrole protons which are unequivalent because of the β-substitution. The pyrrole resonances of (2-OH-TPP)Fe^{III}Cl have nearly equal line widths. The differential broadening of the pyrrole resonances determined for the trimeric molecule is absent. The *meso*-phenyl resonances are observed in the 16−5 ppm region as expected for high-spin iron(III) tetraphenylporphyrin. A unique resonance at 16.0 ppm for (2-OH-TPP)Fe^{III}Cl, and 17.8 ppm for (2-OH-TPP)-Fe^{III}Br has been assigned to the β-hydroxyl proton. When chloroform-*d* saturated with deuterium oxide was added to the solution of (2-OH-TPP)Fe^{III}Cl the 2-OH resonance disappeared (Figure 7, Trace B). Reaction 4 is reversible. Addition of a noncoordinating nitrogen base to (2-OH-TPP)Fe^{III}Cl causes its conversion to $[(2\text{-O-TPP})Fe^{III}]_3$. Thus addition of 2,4,6-collidine to the sample of (2-OH-TPP)Fe^{III}Cl results in the loss of peaks shown in Figure 7 and growth of resonances shown in Figure 3 for $[(2\text{-O-TPP})Fe^{III}]_3$. This trimerization process, followed by ^{1}H NMR, reconstructed selectively the *RRS* and *SSR* diastereoisomers, i.e. the composition of the starting enantiomeric mixture.

The resonance at 79.1 ppm for (2-OH-TPP)Fe^{III}Br has been assigned to the 3-H position at the β-substituted pyrrole by comparison of ^{1}H NMR spectra of (2-OH-TPP)Fe^{III}Br and (2-OH-TPP-d_6)Fe^{III}Br (Figure 7, Trace D). The selective deuteration of all but the 3-H position has been determined for (2-OH-TPP-d_6)Fe^{III}Br. Unexpectedly this unique proton has the shift in a middle of other pyrrole resonances. The noticeable downfield shifts of the 3-H proton were found in other known high-spin β-substituted iron(III) tetraphenylporphyrins: (2-BzO-TPP)Fe^{III}Cl, 91.4 ppm; (2-NO_2-TPP)Fe^{III}Cl, 102.6 ppm; (2-PPh_3-TPP)$Fe^{III}Cl_2$, 103.7 ppm; (2-py-TPP)$Fe^{III}Cl_2$, 95.6 ppm. (298 K).[23,25]

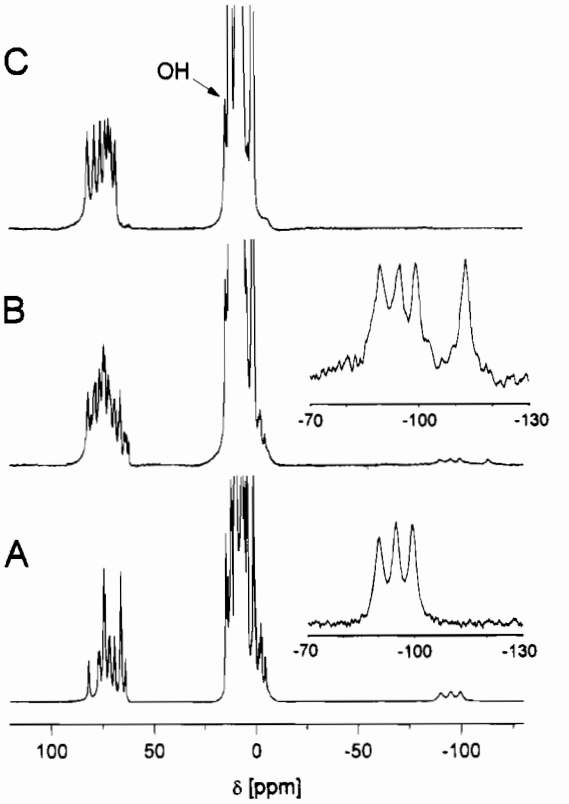

Figure 8. ^{1}H NMR titration of $[(2\text{-O-TPP})Fe^{III}]_3$ with TFA (chloroform-*d*, 291 K). Number of TFA equivalents added: (A) 0; (B) 2; (C) 4. Insets by traces A and B present broad 3-H pyrrole resonances.

Titration of $[(2\text{-O-TPP})Fe^{III}]_3$ with TFA in chloroform-*d* at 291 K produces a gradual growth of a new set of resonances while the resonances of the trimer diminish in intensity. The titration process is presented in Figure 8. The ^{1}H NMR spectrum of the final product (Figure 8, trace C) indicates the formation of the five-coordinate complex (2-OH-TPP)Fe^{III}-(TFA). The overall pattern found for (2-OH-TPP)Fe^{III}Cl and (2-OH-TPP)Fe^{III}Br is retained in the spectrum of (2-OH-TPP)-Fe^{III}(TFA). At lower molar ratios of TFA to the trimer it is possible to detect, apart from $[(2\text{-O-TPP})Fe^{III}]_3$ and (2-OH-TPP)-Fe^{III}(TFA), an intermediate involved in the process of the protic cleavage. Trace B of Figure 8 shows the ^{1}H NMR spectrum obtained by adding 2 equiv of TFA to a solution of $[(2\text{-O-TPP})Fe^{III}]_3$. In the downfield and upfield region new resonances appear that are indicative of the formation of a new, oligomeric high-spin iron(III) complex(es). In particular, the new intense 3-H resonance is readily seen at −112 ppm. The difference spectrum (not shown) obtained by subtracting the spectrum of the upfield pyrrole resonances for $[(2\text{-O-TPP})Fe^{III}]_3$ from the spectrum at trace B presents clearly only one upfield shifted pyrrole resonance at −112 ppm that is characteristic for the single Fe−O−PFe bridging fragment. The general spectral pattern is similar to that described for $[(2\text{-O-TPP})Fe^{III}]_3$, hence another oligomeric species is present. The protic cleavage can produce two linear structures, HO−PFe−O−PFe−O−PFe−TFA and HO−PFe−O−PFe−TFA, before the final conversion into (2-OH-TPP)Fe^{III}(TFA). We discount the linear trimer in

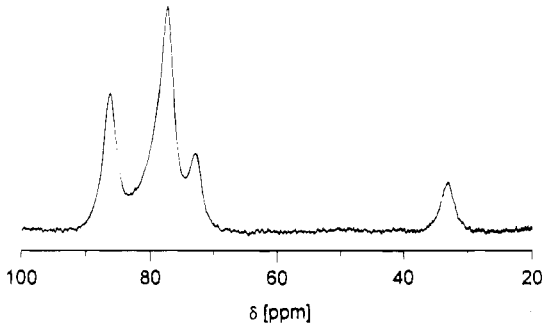

Figure 9. Pyrrole region of the ^{1}H NMR spectrum for [(2-O-TPP)-Fe^{III}]$_3$ in chloroform-*d* solution at 293 K after addition of sodium hydroxide in methanol-d_4.

favor of the dimer because only a single diagnostic 3-H signal, expected for the linear dimeric structure, is apparent.

Formation of Monomeric Complexes by Addition of Bases. Addition of an excess of base (methoxide ion, hydroxide ion in methanolic solutions) to a solution of [(2-O-TPP)Fe^{III}]$_3$ in chloroform-*d* results in its conversion to the five-coordinate, high-spin complex:

$$[(2\text{-O-TPP})Fe^{III}]_3 + 3X^- \rightarrow 3[(2\text{-O-TPP})Fe^{III}X]^- \quad (5)$$

$$X = CH_3O^-, OH^-$$

The effect of adding hydroxide anion is shown in Figure 9. Four downfield resonances of relative intensities 2:3:1:1 are assigned to pyrrole protons. In particular the 3-H resonance occurs at 33.4 ppm (and at 33.7 ppm for the methanolate complex). Its unique position results from the increased contribution of the keto tautomer in the basic conditions (vide infra). Addition of water to the chloroform solution of [(2-O-TPP)Fe^{III}X]$^-$ results in reconversion to the trimer.

Keto−Enol Tautomerism in (2-OH-TPP)Fe^{III}Cl. During the synthesis of the pyrrole-deuterated [(2-O-TPP)Fe^{III}]$_3$, we have observed the increased lability of the 3-H proton. The usual procedure of trimer synthesis has been modified by the replacement of (2-BzO-TPP)Fe^{III}Cl with (2-BzO-TPP-d_7)Fe^{III}-Cl (80% deuteration at pyrrole positions as shown by ^{1}H NMR). The intensity of the upfield shifted pyrrole resonances has been recovered in the ^{1}H NMR spectrum of [(2-O-TPP-d_6)Fe^{III}]$_3$ (not shown) contrary to the reduced intensity of the downfield shifted pyrrole resonances. The acidic cleavage [(2-O-TPP-d_6)Fe^{III}]$_3$, followed by ^{1}H NMR, produced the spectrum of (2-OH-TPP-d_6)Fe^{III}Br with the recovered intensity of the 3-H resonance. (Figure 7, trace D). To account for the process of the deuterium−proton exchange we have considered the keto−enol tautomerism established by Crossley et al. for zinc(II) and copper(II) complexes of 2-hydroxytetraphenylporphyrin.[14] The mechanism, adapted to (2-BzO-TPP-d_7)Fe^{III}Cl, is presented in Scheme 2.

The (2-OH-TPP)Fe^{III}Br complex contains almost entirely the 2-hydroxyporphyrin tautomer because its ^{1}H NMR spectrum demonstrates the hydroxyl resonance. The observation of a proton−deuterium exchange suggests that there is an equilibrium between an enol and keto form of β-substituted iron(III) porphyrin. The observed difference of the 3-H hyperfine shift of (2-OH-TPP)Fe^{III}Br and (2-BzO-TPP)Fe^{III}Cl supports this analysis. The (2-OH-TPP)Fe^{III}Cl and [(2-O-TPP)Fe^{III}(OH)]$^-$ complexes provide spectroscopic models for the hydroxyl and keto tautomeric complexes, respectively.

Conclusions

The self-assembly process of monomeric iron(III) 2-hydroxy-5,10,15,20-tetraphenylporphyrin to form an unprecedented cyclic

Scheme 2

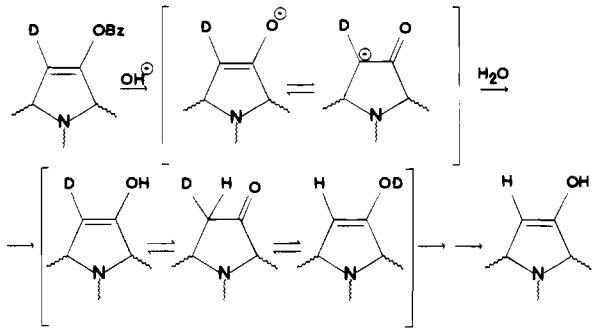

trimeric complex has been established through a variety of spectroscopic investigations. The spectroscopic evidence indicates that the iron(III) complex has a head-to-tail trimeric structure with the pyrrolic-alkoxide groups forming bridges from one macrocycle to the metal in the adjacent macrocycle PFe−OPFe−OPFe−O. The configuration of the trimeric species, formed in the course of oligomerization, depends on the information stored in the optically active monomeric units. The internal structure of the substrate allows to obtain the preferred diastereoisomeric composition of the trimeric product by the molecular recognition. The ^{1}H NMR spectra of iron(III) 2-hydroxytetraphenylporphyrin complexes {(2-OH-TPP)Fe^{III}-Cl and [(2-O-TPP)Fe^{III}]$_3$} presented useful and potentially unique probes for detecting these monomeric and trimeric species in the complex reaction mixtures. In particular the characteristic large pyrrole upfield hyperfine shifts (ca. −90 ppm) provide clear pyrrole signals in the ^{1}H NMR window, which is unique for iron(III) porphyrins. The (2-OH-TPP)Fe^{III}-Cl complex exists almost entirely in the hydroxyl form. However, the base-catalyzed exchange of the proton at the position next to the hydroxy group demonstrated the presence of a tautomer in low equilibrium concentration which has a keto chlorin structure of the ligand.

It occurred to us that 2-hydroxy(oxo)-substituted iron porphyrins might be involved in the degradation of iron porphyrin catalysts in presence of oxidizing substrates including peroxides or peroxyacids. The spectroscopic results of this investigation should be relevant to their identification.

Experimental Section

Solvents and Reagents. All solvents were purified by standard procedures. Tetraphenylporphyrin $TPPH_2$, $TPPH_2$-d_8, and $TPPH_2$-d_{20}, were prepared using reported methods.[41,42] Benzaldehyde-d_5 used in the synthesis of $TPPH_2$-d_{20} was obtained by oxidation of toluene-d_8 with $Ce(NH_4)_2(NO_3)_6$.[43] Chloroform-*d* ($CDCl_3$, Glaser AG) was dried before use by passing through activated basic alumina.

Preparation of Compounds. 2-BzO-$TPPH_2$. (2-Benzoyloxy)-tetraphenylporphyrin was prepared by a standard procedure starting from $TPPH_2$.[4] The β-substituted porphyrin products were chromatographed on a silica gel column (Merck Type 60, 0.015−0.040 mm). Elution with benzene gave several fractions, the second one containing 2-BzO-$TPPH_2$ (identified by ^{1}H NMR), that was recovered as a violet powder after evaporation of the solvent under vacuum. This separation procedure avoided a metal insertion step prior to chromatography. The respective deuterated derivatives were obtained from the deuterated precursors.

(2-BzO-TPP)Fe^{III}Cl. A solution of 200 mg (1 mmol) of iron(II) chloride tetrahydrate in 50 mL of ethanol was added to a solution of 40 mg (0.054 mmol) of (2-benzoyloxy)tetraphenylporphyrin in 100 mL

(41) Lindsey, J. S.; Schreiman, I. C.; Hsu, H. C.; Kearney, P. C.; Marguerettaz, A. M. *J. Org. Chem.* **1987**, *52*, 827.
(42) Boersma, A. D.; Goff, H. M. *Inorg. Chem.* **1982**, *21*, 581.
(43) Syper, L. *Tetrahedron Lett.* **1966**, *37*, 4493.

of chloroform. The solution was heated under reflux for 0.5 h. It was cooled and then solvent was removed on the rotary evaporator. The solid residue was extracted with chloroform. The chloroform solution was subjected to column chromatography on a silica gel column. Elution with chloroform gave the fraction containing 2-BzO-TPPH$_2$. Further elution with chloroform/methanol (97:3 v/v) produced a brownish fraction. The product was identified by means of electronic and ^{1}H NMR spectroscopy as a μ-oxo-bridged complex, [(2-BzO-TPP)-Fe^{III}]$_2$O. Hydrogen chloride in dichloromethane was added to the solution of [(2-BzO-TPP)Fe^{III}]$_2$O in dichloromethane. The solution was evaporated to dryness, and recrystallized from dichloromethane/*n*-hexane; yield 98%. UV−vis (CH_2Cl_2), λ_{max} (log ϵ): 418 (4.99), 510 (4.10), 579 (3.52), 660 sh, 688 nm (3.43).

The selectively deuterated derivatives were synthesized analogously from the corresponding deuterated (2-benzoyloxy)porphyrins to produce (2-BzO-TPP-d_{20})Fe^{III}Cl and (2-BzO-TPP-d_7)Fe^{III}Cl.

[(2-O-TPP)Fe^{III}]$_3$. (2-BzO-TPP)Fe^{III}Cl or [(2-BzO-TPP)Fe^{III}]$_2$O (30 mg) was dissolved in 50 mL of ethanol and heated under reflux. The pellets of NaOH were added to this solution. The color changed from brown to brown-green. The heating was discontinued after 15 min. The reaction mixture was diluted with benzene and washed several times with aqueous NaOH and water. The organic layer was separated, dried with anhydrous magnesium sulfate. The solid material was filtered off and the filtrate was evaporated to dryness on the rotary evaporator. The dichloromethane solution of the solid residue was subjected to chromatography on a basic alumina column. Elution with dichloromethane gave the green-brown fraction that was recovered as the solvent was removed under vacuum. Recrystallization of this solid from dichloromethane/*n*-hexane (1/1 v/v) produced [(2-O-TPP)Fe^{III}]$_3$, which precipitated as the violet powder, yield 70−80%.

UV−vis spectrum (CH_2Cl_2), λ_{max} (log ϵ, per iron porphyrin unit): 408 (Soret, 4.64), 500 (3.96), 625 (3.69), 640 nm (3.67). MS (LSIMS): $(m + 1)/Z = 2050$. Anal. Calcd for $C_{132}H_{81}N_{12}O_3Fe_3$: C, 77.31; H, 3.98; N, 8.20. Found: C, 77.30; H, 4.11; N, 8.02.

[(2-O-TPP-d_6)Fe^{III}]$_3$ and [(2-O-TPP-d_{20})Fe^{III}]$_3$ were synthesized following the procedure elaborated for [(2-O-TPP)Fe^{III}]$_3$.

(2-OH-TPP)Fe^{III}Cl. Hydrogen chloride in dichloromethane was added to the solution of [(2-O-TPP)Fe^{III}]$_3$ in dichloromethane (the color changed from green-brown to red-brown). The solution was evaporated to dryness and the solid residue recrystallized from dichloromethane/*n*-hexane (1/1 v/v).

UV−vis (CH_2Cl_2), (log ϵ): 419 (Soret, 4.80), 510 (3.96), 580 (3.46), 670 nm (3.44).

The bromo derivative was prepared by stirring the dichloromethane solution of [(2-O-TPP)Fe^{III}]$_3$ with 1 M aqueous HBr. The organic layer was separated, dried, and evaporated to dryness, yielding (2-OH-TPP)-Fe^{III}Br as a violet powder.

Cleavage Procedures. Solutions of known concentration (2−3 mM in chloroform-*d* for ^{1}H NMR, 0.01−0.1 mM in dichloromethane for UV−vis spectroscopy) of the trimeric complex [(2-O-TPP)Fe^{III}]$_3$ were prepared. The respective solution of the cleaving reagent (trifluoroacetic acid in chloroform-*d*, NaOH in methanol-d_4, or CD_3ONa in methanol-d_4) was titrated by a syringe, and the progress of the reaction was monitored by ^{1}H NMR or UV−vis spectroscopy.

Molecular Mechanics Calculation. Molecular mechanics calculations using the HyperChem software (Autodesk) were carried out and displayed on a PC 486 computer. The standard MM+ force field, with the constraints set on the coordination bonds to achieve a high-spin iron(III) porphyrin geometry, have been used as described in the text.

Instrumentation. ^{1}H NMR spectra were recorded on a Bruker AMX spectrometer operating in the quadrature mode at 300 MHz. A typical spectrum was collected over a 45 000 Hz spectral window with 16K data points with 500−5000 transients for the experiment and a 50 ms prepulse delay. The free induction decay (FID) was apodized using exponential multiplication depending on the natural line width. This induced 5−50 Hz broadening. The residual ^{1}H NMR resonances of the deuterated solvents were used as a secondary reference. An inversion−recovery sequence was used to suppress the diamagnetic signals in the selected spectra. The ^{2}H NMR spectra were collected using a Bruker AMX instrument operating at 46.1 MHz. A spectral width of 20 kHz was typical, and 16K points was used. A pulse delay of 50 ms was applied. The signal to noise ratio was improved similarly as in proton spectra. The residual ^{2}H NMR resonances of the solvents were used as a secondary reference.

Absorption spectra were recorded on a Specord M-42 spectrometer and a diode array Beckman 7500 spectrometer. ESR spectra were measured at the X-band on a SE/X Radiopan spectrometer. Infrared spectra were recorded on a Specord M-80 spectrometer using KBr pellets. Mössbauer spectra were measured with a MS 2320 POLON spectrometer equipped with a ^{57}Co (Cr matrix) source. Mass spectra were recorded on a ADM-604 spectrometer using the liquid matrix secondary ion mass spectrometry technique and a primary beam of 8 keV Cs^+ ions. A Bruker 300 AMX spectrometer was used for magnetic susceptibility measurements by the Evans technique in solution using the peak of hexamethyldisiloxane as a reference.[29] Diamagnetic corrections were obtained by using published values of for constitutive corrections for TPPH$_2$[44] and Pascal's constants.

Acknowledgment. The financial support of the State Committee for Scientific Research KBN (Grant 2 2651 92 03) is kindly acknowledged.

IC9405081

(44) Eaton, S.; Eaton, G. R. *Inorg. Chem.* **1980**, *19*, 1095.